Phonon anharmonicity in silicon from 100 to 1500 K

D. S. Kim,[1,*] H. L. Smith,[1] J. L. Niedziela,[2] C. W. Li,[3] D. L. Abernathy,[4] and B. Fultz[1]

[1]*Department of Applied Physics and Materials Science, California Institute of Technology, Pasadena, California 91125, USA*
[2]*Instrument and Source Division, Oak Ridge National Laboratory, Oak Ridge, Tennessee 37831, USA*
[3]*Materials Science and Technology Division, Oak Ridge National Laboratory, Oak Ridge, Tennessee 37831, USA*
[4]*Quantum Condensed Matter Division, Oak Ridge National Laboratory, Oak Ridge, Tennessee 37831, USA*

Inelastic neutron scattering was performed on silicon powder to measure the phonon density of states (DOS) from 100 to 1500 K. The mean fractional energy shifts with temperature of the modes were $\langle \Delta \varepsilon_i / \varepsilon_i \Delta T \rangle = -0.07$, giving a mean isobaric Grüneisen parameter of $+6.95 \pm 0.67$, which is significantly different from the isothermal parameter of $+0.98$. These large effects are beyond the predictions from quasiharmonic models using density functional theory or experimental data, demonstrating large effects from phonon anharmonicity. At 1500 K the anharmonicity contributes $0.15 k_B$/atom to the vibrational entropy, compared to $0.03 k_B$/atom from quasiharmonicity. Excellent agreement was found between the entropy from phonon DOS measurements and the reference NIST-JANAF thermodynamic entropy from calorimetric measurements.

I. INTRODUCTION

Phonons are responsible for most of the entropy of materials at modest temperatures. The phonon entropy, or vibrational entropy, can be estimated with a set of fixed phonon frequencies in the harmonic approximation, but these results are usually too inaccurate for thermodynamic predictions of phase stability at elevated temperatures [1]. Changes in phonon frequencies with temperature are generally important for calculating thermodynamic functions [2], but our understanding of high-temperature behavior is still emerging. Such studies require phonon spectra at high T, for which there are few experimental data.

The thermal properties of silicon are of importance for silicon-based electronics, nanomechanics, photovoltaics, thermoelectrics, and batteries [3–11]. Some of the nonharmonic behavior of a material is expected to originate from "quasiharmonic" thermal softening (reduction in frequency) of phonons, where the phonon entropy increases as the material expands against its bulk modulus. Anharmonicity from phonon-phonon interactions causes further phonon softening without thermal expansion and can account for a substantial part of the entropy of materials at high temperatures. Anharmonic phonon-phonon interactions also shorten the lifetimes of phonons, causing broadenings in the phonon spectrum and a finite phonon mean free path for thermal transport.

The lattice dynamics of silicon has attracted ongoing attention owing to its anomalous thermal expansion, which changes from negative to positive at low temperatures. Phonon dispersions of silicon have been reported, as have phonon densities of states (DOS), thermal properties, and mode Grüneisen parameters [12–17]. The work with density functional theory (DFT) on silicon includes one of its earliest successes for determining the crystal structure of a solid at elevated temperatures [18]. Experimental work has employed inelastic neutron scattering (INS) and Raman spectroscopy up to 300 K and to high pressures [12–14,19–23]. These studies assessed

and correctly described the low-temperature lattice dynamics, but to our knowledge there has not been a study of phonons in silicon by inelastic neutron scattering at temperatures above 700 K. Measurements at higher temperatures are important for assessing phonon anharmonicity, which is also pertinent to thermal conductivity at all temperatures.

In the present work we measured phonon DOS curves on high-purity silicon powder using a direct geometry inelastic neutron spectrometer and investigated the phonon DOS with DFT. We found that the thermal changes in phonon frequencies were a factor of 7 larger than expected from the quasiharmonic model, indicating a large effect from phonon anharmonicity. The thermal broadening of features in the phonon spectrum also indicates anharmonicity.

II. METHODS

A. Inelastic neutron scattering

Inelastic neutron scattering (INS) spectra were obtained with ARCS [24], a time-of-flight Fermi chopper spectrometer at the Spallation Neutron Source at Oak Ridge National Laboratory, using an incident energy of 97.5 meV and an oscillating radial collimator to reduce background and multiple scattering [25]. Silicon of 99.9999% purity was pulverized, and 7.9 g of powder with an effective sample thickness of 6.0 mm were contained in an aluminum sachet and mounted in a closed-cycle helium refrigerator for measurements at temperatures of 100, 200, and 300 K. Similar sachets made of niobium foil were mounted in a low-background electrical resistance vacuum furnace for measurements at temperatures of 301, 600, 900, 1000, 1100, 1200, 1300, 1400, and 1500 K. Backgrounds were measured on empty sachets in the same sample environment at corresponding temperatures. Time-of-flight neutron data were reduced with the standard software packages in the procedures for the ARCS instrument as described previously [26–28]. Data reduction included subtraction of the background and corrections for multiple scattering and multiphonon scattering. Because silicon is a coherent scatterer, averages over a wide range of momentum
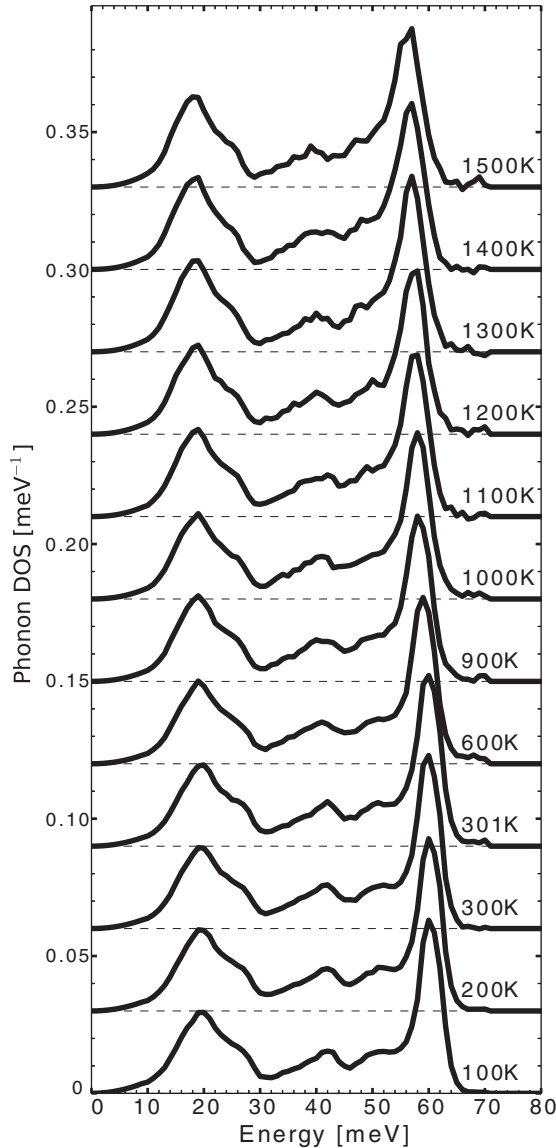
* dskim@caltech.edu

FIG. 1. Phonon DOS curves of silicon $g_T(\varepsilon)$ normalized to unity. Curves are offset for clarity.

transfer (2–12 Å^{-1}) were used to obtain the phonon DOS curves presented in Fig. 1. Successful background subtraction is indicated by the close similarity of the room-temperature measurements in both the closed-cycle refrigerator and the electrical resistance furnace (300 and 301 K).

B. *Ab initio* calculations

Ab initio DFT and density functional perturbation theory (DFPT) calculations were performed with the VASP package [29–33]. The generalized gradient method was used with Perdew-Burke-Ernzerhof (PBE) exchange correlation functionals [34,35] for projector-augmented-wave pseudopotentials [36,37] and a plane-wave basis set. All calculations used a kinetic-energy cutoff of 500 meV, a direct supercell of 216 atoms, and a $2 \times 2 \times 2$ k-point grid. The energy cutoffs, k-point density, and configurations were converged to within 5 meV/atom. The phonon eigenenergies were computed

through DFPT [33,38]. The free energy was calculated as

$$
\begin{aligned}
F(T,V) = \ & E_0(V) \\
& + \int d\varepsilon \ g(\varepsilon) \left[\frac{\varepsilon}{2} + k_{\mathrm{B}} T \ln(1 - e^{-\varepsilon/k_{\mathrm{B}}T}) \right]. \quad (1)
\end{aligned}
$$

The quasiharmonic approximation (QHA) calculations were obtained by minimizing the free energy $F(T, V\{a_0\})$ of Eq. (1) with respect to the volume of the supercell. Ground-state energies $E_0(V)$ were calculated separately and self-consistently for each volume, and the DOS $g(\varepsilon)$ were calculated with the specific lattice parameter, a_0, that produced the minimized volume.

III. RESULTS

A sharp cutoff of the phonon spectrum occurs at 67 meV. The phonon DOS are near zero well above this cutoff, indicating the success of the corrections for background, multiple scattering, and multiphonon scattering. Figure 1 shows that the phonon DOS go through a systematic thermal softening (decrease in phonon energy) and thermal linewidth broadening with increasing temperature. The DOS curves contain five distinct features caused by Van Hove singularities. At 300 K, two transverse acoustic modes between 10 and 30 meV give the peak near 18 meV and the shoulder near 26 meV. The two features between 30 and 55 meV are from longitudinal acoustic and optical modes, respectively. Finally, the higher-energy feature around 60 meV is from transverse and longitudinal optical modes. The high-energy optical modes centered around 60 meV show the largest thermal shift of approximately 4 meV between 100 and 1500 K, but the largest fractional changes $\Delta\varepsilon_i/\varepsilon_i$ are found for the low-energy transverse acoustic modes from 10 to 30 meV. The negative fractional shifts of the five features are shown in Fig. 2. Fractional shifts agree within $\pm 1\%$ of the average fractional shift. This uniform trend might seem to be indicative of a simple quasiharmonic behavior, but the magnitude of the shift proves to be too large.

The measured DOS agree strongly with the calculations and allow for the identification of the five distinct features in the DOS corresponding to the specific branch or branches in the silicon dispersion relations as seen in Fig. 3. The phonon dispersion and DOS (Fig. 3) were calculated in the QHA at the 100 K equilibrium volume and scaled in energy to fit the 100 K measured DOS. Each branch was labeled and identified according to previously reported methods and results [12,39].

The self-similarity of the phonon DOS at elevated temperatures is shown in Fig. 4. Here the phonon DOS measured at 100 K was rescaled in energy and normalized to unity.

$$
g'(\varepsilon) = g_{100K}\{[1 - 3\alpha_T \bar{\gamma}_T(T - 100)]\varepsilon\}. \quad (2)
$$

The rescaled phonon DOS $g'(\varepsilon)$ is shown with the experimental DOS curve for 1500 K. The thermal expansion coefficient α and isobaric Grüneisen parameter are defined later in the text [Eq. (6)]. The two curves are in good coincidence, although the thermal broadening of the longitudinal peak at 56 meV is evident.

In the quasiharmonic approximation, the minimization of the free energy of Eq. (1) gives γ_i, the mode Grüneisen
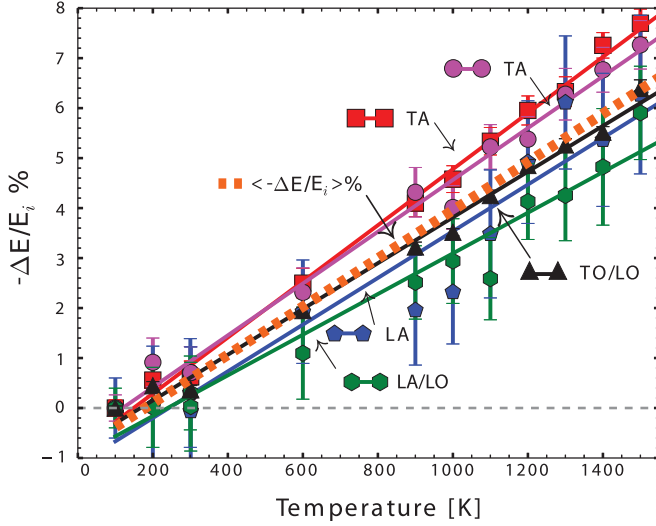
FIG. 2. (Color online) The negative of the fractional thermal shifts of the five features of the DOS: transverse acoustic (TA; red squares and purple circles), longitudinal acoustic (LA; blue pentagons), longitudinal acoustic and optical (LA/LO; green hexagons), and transverse and longitudinal optical modes (TO/LO; black triangles). The average between the shifts of the five features is shown by a dotted orange line.

parameter,

$$\gamma_i \equiv -\frac{V}{\varepsilon_i}\frac{\partial \varepsilon_i}{\partial V}, \quad (3)$$

defined as the fractional shift of energy of phonon mode i per fractional shift in volume. There have been many studies defining the Grüneisen parameter as mode specific [14,17,40,41], but from the uniform thermal behavior of the phonons in the whole Brillouin zone, we present a mean Grüneisen parameter in Table I, defined as

$$\bar{\gamma} = -\left\langle \frac{V}{\varepsilon_i}\frac{\Delta \varepsilon_i}{\partial V}\right\rangle = -\left\langle \frac{\partial \ln \varepsilon_i}{\partial \ln V}\right\rangle. \quad (4)$$
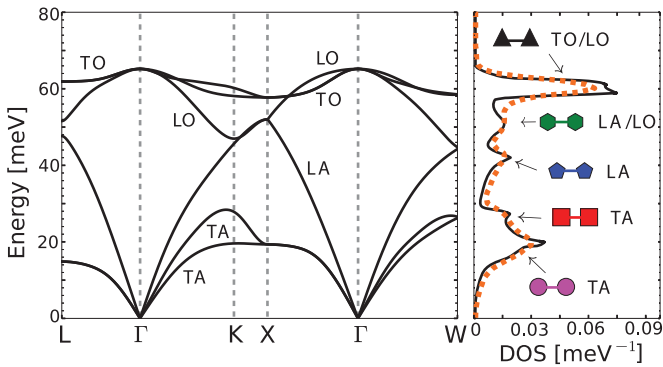

FIG. 3. (Color online) Phonon dispersion and DOS of silicon at the quasiharmonic 100 K equilibrium volume (black solid line) scaled in energy to fit the experimental 100 K DOS (orange dotted line) from Fig. 1. The distinct features are labeled with the corresponding markers used in Fig. 2.
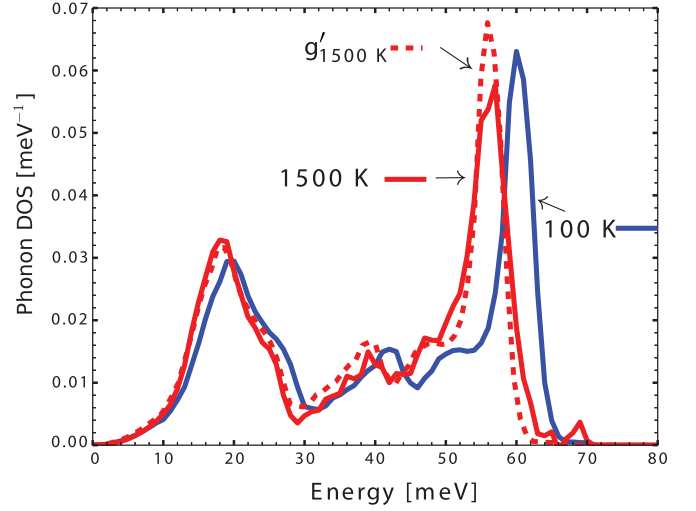

FIG. 4. (Color online) Silicon phonon DOS of experimental measurements at 100 K (blue solid line) and 1500 K (red solid line). A DOS at 1500 K (red dotted line) is obtained from shifting and renormalizing the measured DOS at 100 K [Eq. (2)].

The isothermal ($\bar{\gamma}_P$) and isobaric ($\bar{\gamma}_T$) Grüneisen parameters are defined as

$$\bar{\gamma}_P = -\frac{1}{3\alpha(T)}\left\langle \frac{\partial \ln \varepsilon_i}{\partial V}\right\rangle\bigg|_T \frac{\partial V}{\partial T} = B_T \left\langle \frac{\partial \ln \varepsilon_i}{\partial P}\right\rangle\bigg|_T, \quad (5)$$

$$\bar{\gamma}_T = -\frac{1}{3\alpha(T)}\left\langle \frac{\partial \ln \varepsilon_i}{\partial T}\right\rangle\bigg|_P, \quad (6)$$

$$\bar{\gamma}_T = -\frac{1}{3\alpha(T)}\left(\left\langle \frac{\partial \ln \varepsilon_i}{\partial V}\right\rangle\bigg|_T \frac{\partial V}{\partial T} + \left\langle \frac{\partial \ln \varepsilon_i}{\partial T}\right\rangle\bigg|_V\right), \quad (7)$$

$$\bar{\gamma}_T = \bar{\gamma}_P - \frac{1}{3\alpha(T)}\left\langle \frac{\partial \ln \varepsilon_i}{\partial T}\right\rangle\bigg|_V. \quad (8)$$

The isothermal and isobaric parameters describe the phonon energy shifts from effects of temperature and volume, where $\alpha(T)$ is the coefficient of linear thermal expansion and B_T is the bulk modulus. The experimental phonon shifts shown in Fig. 2 were used to obtain $\bar{\gamma}_T$ with Eq. (6), whereas all of the QHA parameters used phonon energy shifts from the differences in DFPT-calculated DOS of the change in volume that minimized the free energy [Eq. (1)]. From Eq. (8), $\bar{\gamma}_T$ contains not only a contribution from the volume-dependent phonon frequency shifts, the "quasiharmonic" contribution, but also a second term from a pure temperature dependence, the

TABLE I. Calculated and measured Grüneisen parameters using constants at room temperature. See text for details on values and method of calculation. Note that error bars were calculated from the differences in peak shifts of the five features.

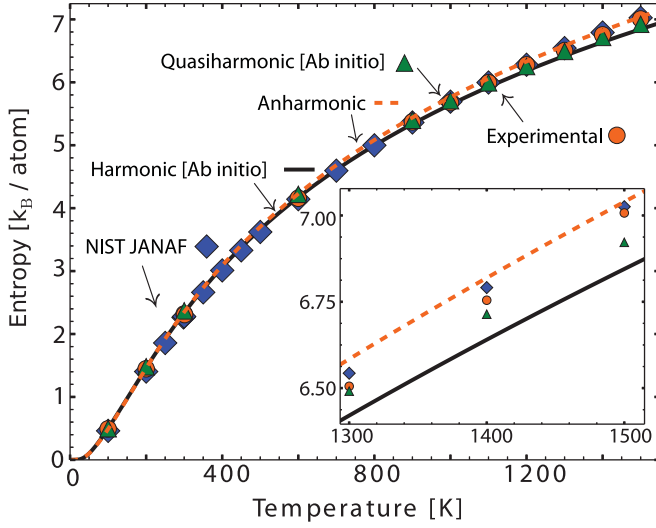|	Experiment	Calculated in the QHA
$\bar{\gamma}$		1.00 ± 0.60
$\bar{\gamma}_T$	7.00 ± 0.67	1.102 ± 0.72
$\bar{\gamma}_P$	0.98	
γ	0.367	

FIG. 5. (Color online) Vibrational entropy of silicon from experimental phonon DOS curves (orange circles). Entropy from calculated DOS curves are also shown: harmonic (solid black line) and quasiharmonic (green triangles). The interpolated anharmonic approximation is shown (orange dotted line), as is the NIST-JANAF entropy data (blue diamonds) [46]. The inset enlarges the high-temperature region.

"anharmonic" contribution. The calculated isobaric and isothermal parameters were normalized with room-temperature thermal expansion coefficients for consistency. Coefficients of linear thermal expansion $\alpha(T)$ were obtained from reported values of thermal expansion and lattice constants [42,43]. Our experimental isobaric parameter $\bar{\gamma}_P$ was calculated using Eq. (5) with phonon shifts from high-pressure Raman spectroscopy measurements reported by Weinstein and Piermarini [23]. The thermodynamic Grüneisen parameter γ is defined as

$$\gamma = \frac{3\alpha V_0 B_T}{C_V} \quad (9)$$

and is listed in Table I. It was evaluated with $B_T = 0.9784 \times 10^{11}$ Pa [44], $\alpha = 2.59 \times 10^{-6}$ K^{-1} [44], and the classical result of heat capacity [1], $C_V = 25$ J/(mol K). Table I shows a large discrepancy between $\bar{\gamma}_T$ from the phonon measurements and the Grüneisen parameters from volume expansion.

To first order, the phonon DOS is the only function needed to obtain the vibrational entropy [1,45]

$$S_{\text{vib}}(T) = 3k_B \int d\varepsilon \, g(\varepsilon)[(n+1)\ln(n+1) - n\ln(n)]. \quad (10)$$

The entropy $S_{\text{vib}}(T)$ obtained from each measured DOS at temperature T, $g(\varepsilon)(T)$, is shown by orange circles in Fig. 5. To obtain a continuous curve, we also calculated the entropy with rescaled DOS curves from Eq. (2), using the experimental $\bar{\gamma}_T = 7.0$ from Table I. An *ab initio* calculation of a DOS at 0 K is used with Eq. (10) to obtain a harmonic entropy for all temperatures. For the calculated results in the QHA, the *ab initio* DOS with thermal expansion were evaluated. At the highest measured temperature of 1500 K, we find that the anharmonic contribution to entropy is 0.15k_B/atom, which is a factor of 5 larger than the quasiharmonic entropy

contribution of 0.03k_B/atom. Finally, the total entropy from the National Institute of Standards and Technology-Joint Army Navy Air Force (NIST-JANAF) database [46] is shown in Fig. 5.

IV. DISCUSSION

At all temperatures, the vibrational entropy $S_{\text{vib}}(T)$ obtained from the experimental phonon DOS measurements is in excellent agreement with the total entropy from the JANAF tables (Fig. 5). The agreement to within approximately 1% is striking, especially considering that the JANAF tables were assessed from calorimetric measurements and our $S_{\text{vib}}(T)$ was obtained by counting phonons. The JANAF entropy is slightly higher than the phonon entropy at high temperatures, suggesting an additional contribution, but the reliability of this difference is not yet understood. The contribution from electron excitations is probably negligible, and we also expect the phonon spectrum will be little affected by adiabatic electron-phonon coupling [1,45,47–49].

A harmonic model accounts for most of the entropy of silicon at modest temperatures, but the error at high temperatures is thermodynamically significant. The first correction from the quasiharmonic approximation is small because the bulk modulus is modest, and the thermal expansion is small for strongly covalently bonded atoms [14]. Both the measured and calculated mode-specific Grüneisen parameters have variations but are approximately 1 at elevated temperatures [17,41]. Prior calculations of temperature-dependent Grüneisen parameters in the quasiharmonic approximation also do not exceed 1 [14]. Much of the previous interest in the lattice dynamics of silicon was centered on its peculiar thermal expansion at cryogenic temperatures. At low temperatures and high pressures, the quasiharmonic approximation has predicted accurate thermophysical behavior [14,17,20]. The quasiharmonic model predicts the thermal expansion at low temperatures well and predicts the thermal expansion at high temperatures adequately [50]. The low-energy transverse modes in the open diamond cubic crystal structure have been suggested as the source of the low-temperature negative thermal expansion [20,51,52], but the mechanistic details are not fully understood. Nevertheless, it is possible that the openness of the diamond cubic structure may also be responsible for the anharmonicity and low thermal expansion of silicon when all of the phonon modes are highly populated (above 800 K).

Thermal expansion is not a validation of the quasiharmonic model, as it predicts phonon shifts that are in error by an order of magnitude when actual values of thermal expansion are used, as seen by the discrepancy between the experimental and calculated $\bar{\gamma}_T$ in Table I and by the tiny phonon shifts predicted by the quasiharmonic model (e.g., [50]). The failure of the quasiharmonic approximation at high T stems from the assumptions that phonons are noninteracting. Thermal broadening is evident in the peak from longitudinal acoustic modes at 39 meV and longitudinal optic modes at 56 meV at high temperatures. Although lifetime broadening has no effect on the vibrational entropy to first order, we should expect that other anharmonic corrections to the phonon self-energy from the cubic and quartic parts of the phonon

potentials may be important [45]. This is most evident in the differences between $\bar{\gamma}_P$ and $\bar{\gamma}_T$ in Table I. The second term in Eq. (8) for $\bar{\gamma}_T$, which gives the pure temperature dependence of the phonon energy, is much larger than the first term from the quasiharmonic contribution. This pure anharmonicity dominates the nonharmonic thermodynamics of silicon at high temperatures, where 80% of the deviation from the harmonic model is from pure anharmonicity. If the phonon shifts (Fig. 2) were only dependent on volume changes and excluded temperature effects, the mode Grüneisen parameter $\bar{\gamma}$ would have a value of around 4.4 when using experimental lattice parameters [42,43]. This is more than a factor of 4 larger than the previously measured isothermal parameters γ_P found in Table I, showing the need to differentiate between the isothermal and isobaric parameters. The experimental points were obtained with Eq. (10), which was derived for noninteracting harmonic or quasiharmonic phonons. With phonon lifetime broadening, there is a net shift of spectral weight to higher frequencies, lowering the apparent vibrational entropy. A small correction for this effect was suggested recently [2], and using this correction for the thermal broadening of the present data would give an upward shift of the experimental points in Fig. 5 by 0.015/atom at 1500 K but less at lower temperatures.

The phonon DOS of silicon shows a curious self-similarity. With increasing temperature the phonon DOS keeps approximately the same shape but is rescaled in energy. The simplest explanation is that all interatomic force constants decrease proportionately with temperature, but this explanation may be specious. At 1500 K the different features of the phonon DOS are broadened differently, reflecting differences in the imaginary part of the phonon self-energy from cubic terms in the phonon potential [45]. Such differences were reported recently by Hellman and Abrikosov [40], who showed large broadenings of the longitudinal and highest optical modes compared to the lower-energy transverse acoustic modes. The different cubic anharmonicities also contribute different real shifts to the phonon self-energies, so a thermal rescaling of force constants would require compensating contributions from the quartic and quasiharmonic contributions of different phonons. It therefore seems unlikely that this self-similarity of the phonon DOS could be precisely accurate, and the different slopes in Fig. 2 suggest that it is only approximate.

V. CONCLUSION

Measurements of the phonon DOS of silicon from 100 to 1500 K showed significant thermal softening and some thermal broadening. From prior experimental studies of the effect of pressure on the phonons and from the present computational study on the effect of volume on phonon frequencies, the quasiharmonic contribution to the nonharmonicity was obtained. At low temperatures, the quasiharmonic model works well to describe the phonon shifts, but at high temperatures all of the thermal broadening and 80% of the thermal softening were due to phonon anharmonicity. Nevertheless, the vibrational entropy calculated from the experimental phonon DOS curves of silicon was found to be within 1% of the total thermodynamic entropy from calorimetry data.

[1] B. Fultz, Prog. Mater. Sci. **55**, 247 (2010).

[2] M. Palumbo, B. Burton, A. CostaeSilva, B. Fultz, B. Grabowski, G. Grimvall, B. Hallstedt, O. Hellman, B. Lindahl, A. Schneider, P. E. A. Turchi, and W. Xiong, Phys. Status Solidi B **251**, 14 (2014).

[3] M. A. Green, J. Zhao, A. Wang, P. J. Reece, and M. Gal, Nature (London) **412**, 805 (2001).

[4] A. I. Hochbaum, R. Chen, R. D. Delgado, W. Liang, E. C. Garnett, M. Najarian, A. Majumdar, and P. Yang, Nature (London) **451**, 163 (2008).

[5] Y. Cui, Z. Zhong, D. Wang, W. U. Wang, and C. M. Lieber, Nano Lett. **3**, 149 (2003).

[6] J. Graetz, C. C. Ahn, R. Yazami, and B. Fultz, Electrochem. Solid State Lett. **6**, A194 (2003).

[7] A. I. Boukai, Y. Bunimovich, J. Tahir-Kheli, J.-K. Yu, W. A. Goddard, III, and J. R. Heath, Nature (London) **451**, 168 (2008).

[8] K. D. Hirschman, L. Tsybeskov, S. P. Duttagupta, and P. M. Fauchet, Nature (London) **384**, 338 (1996).

[9] H. A. Atwater and A. Polman, Nat. Mater. **9**, 205 (2010).

[10] B. Tian, X. Zheng, T. J. Kempa, Y. Fang, N. Yu, G. Yu, J. Huang, and C. M. Lieber, Nature (London) **449**, 885 (2007).

[11] K. E. Petersen, Proc. IEEE **70**, 420 (1982).

[12] G. Nilsson and G. Nelin, Phys. Rev. B **6**, 3777 (1972).

[13] G. Dolling and R. A. Cowley, Proc. Phys. Soc. **88**, 463 (1966).

[14] S. Wei, C. Li, and M. Y. Chou, Phys. Rev. B **50**, 14587 (1994).

[15] C. Flensburg and R. F. Stewart, Phys. Rev. B **60**, 284 (1999).

[16] G. Lang, K. Karch, M. Schmitt, P. Pavone, A. P. Mayer, R. K. Wehner, and D. Strauch, Phys. Rev. B **59**, 6182 (1999).

[17] W. B. Gauster, Phys. Rev. B **4**, 1288 (1971).

[18] M. T. Yin and M. L. Cohen, Phys. Rev. B **26**, 5668 (1982).

[19] J. Kulda, D. Strauch, P. Pavone, and Y. Ishii, Phys. Rev. B **50**, 13347 (1994).

[20] S. Biernacki and M. Scheffler, Phys. Rev. Lett. **63**, 290 (1989).

[21] P. Mishra and K. P. Jain, Phys. Rev. B **62**, 14790 (2000).

[22] J. Menéndez and M. Cardona, Phys. Rev. B **29**, 2051 (1984).

[23] B. A. Weinstein and G. J. Piermarini, Phys. Rev. B **12**, 1172 (1975).

[24] D. L. Abernathy, M. B. Stone, M. J. Loguillo, M. S. Lucas, O. Delaire, X. Tang, J. Y. Y. Lin, and B. Fultz, Rev. Sci. Instrum. **83**, 015114 (2012).

[25] M. B. Stone, J. L. Niedziela, M. J. Loguillo, M. A. Overbay, and D. L. Abernathy, Rev. Sci. Instrum. **85**, 085101 (2014).

[26] MANTID, http://www.mantidproject.org/.

[27] M. Kresch, M. Lucas, O. Delaire, J. Y. Y. Lin, and B. Fultz, Phys. Rev. B **77**, 024301 (2008).

[28] M. Kresch, O. Delaire, R. Stevens, J. Y. Y. Lin, and B. Fultz, Phys. Rev. B **75**, 104301 (2007).

[29] G. Kresse and J. Furthmüller, Comput. Mater. Sci. **6**, 15 (1996).

[30] G. Kresse and J. Hafner, Phys. Rev. B **47**, 558 (1993).

[31] G. Kresse and J. Hafner, Phys. Rev. B **49**, 14251 (1994).

[32] G. Kresse and J. Furthmüller, Phys. Rev. B **54**, 11169 (1996).

[33] X. Gonze and C. Lee, Phys. Rev. B **55**, 10355 (1997).

[34] J. P. Perdew, K. Burke, and M. Ernzerhof, Phys. Rev. Lett. **77**, 3865 (1996).

[35] J. P. Perdew, K. Burke, and M. Ernzerhof, Phys. Rev. Lett. **78**, 1396 (1997).

[36] G. Kresse and D. Joubert, Phys. Rev. B **59**, 1758 (1999).

[37] P. E. Blöchl, Phys. Rev. B **50**, 17953 (1994).

[38] A. Togo, F. Oba, and I. Tanaka, Phys. Rev. B **78**, 134106 (2008).

[39] S. Wei and M. Y. Chou, Phys. Rev. B **50**, 2221 (1994).

[40] O. Hellman and I. A. Abrikosov, Phys. Rev. B **88**, 144301 (2013).

[41] A. Beattie and J. Schirber, Phys. Rev. B **1**, 1548 (1970).

[42] Y. Okada and Y. Tokumaru, J. Appl. Phys. **56**, 314 (1984).

[43] D. N. Batchelder and R. O. Simmons, J. Chem. Phys. **41**, 2324 (1964).

[44] R. Hull and INSPEC (Information service), *Properties of Crystalline Silicon* (INSPEC, the Institution of Electrical Engineers, London, 1999).

[45] D. C. Wallace, *Thermodynamics of Crystals* (Dover, Mineola, NY, 1998).

[46] M. W. J. Chase, *NIST-JANAF Thermochemical Tables*, 4th ed. (AIP, New York, 1998).

[47] G. Grimvall, *The Electron-Phonon Interaction in Metals*, Selected Topics in Solid State Physics Vol. 16 (North-Holland, New York, 1981).

[48] O. Delaire, K. Marty, M. B. Stone, P. R. Kent, M. S. Lucas, D. L. Abernathy, D. Mandrus, and B. C. Sales, Proc. Natl. Acad. Sci. **108**, 4725 (2011).

[49] G. Grimvall, *Thermophysical Properties of Materials*, rev. ed. (Elsevier, Amsterdam, Netherlands, 1999).

[50] Z.-K. Liu, Y. Wang, and S. Shang, Sci. Rep. **4**, 7043 (2014).

[51] J. S. Shah and M. E. Straumanis, Solid State Commun. **10**, 159 (1972).

[52] D. F. Gibbons, Phys. Rev. **112**, 136 (1958).